



Hydrophobisation of lignocellulosic materials part I: physical modification

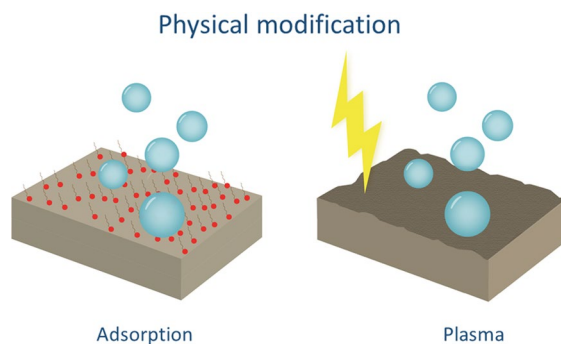
Sandra Rodríguez-Fabià ·
Jonathan Torstensen · Lars Johansson ·
Kristin Syverud

Received: 13 December 2021 / Accepted: 25 April 2022 / Published online: 25 May 2022
© The Author(s) 2022

Abstract This review is the first part of a comprehensive review of hydrophobisation of lignocellulosic materials. The purpose of this review has been to compare physical hydrophobisation methods of lignocellulosic materials. We have compared molecular physical adsorption with plasma etching and grafting. Adsorption methods are facile and rely upon the simple mixing or coating of the substrate with the hydrophobing agent. However, none of the surfactant-based methods reviewed here reach contact angles above 90° , making them unsuitable for applications where a high degree of hydrophobisation is required. Nevertheless, surfactant based methods are well suited for compatibilising the lignocellulosic material with a hydrophobic matrix/polymer in cases where only a slight decrease in the hydrophilicity of the lignocellulosic substrate is required. On the other hand, wax- and lignin-based coatings can provide high hydrophobicity to the substrates. Plasma etching requires a more complex set-up but is relatively cheap. By physically etching the surface with or without the deposition of a hydrophobic

coating, the material is rendered hydrophobic, reaching contact angles well above 120° . A major drawback of this method is the need for a plasma etching set-up, and some researchers co-deposit fluorine-based layers, which have a negative environmental impact. An alternative is plasma grafting, where single molecules are grafted on, initiated by radicals formed in the plasma. This method also requires a plasma set-up, but the vast majority of hydrophobic species can be grafted on. Examples include fatty acids, silanes and alkanes. Contact angles well above 110° are achieved by this method, and both fluorine and non-toxic species may be used for grafting.

Graphical abstract



S. Rodríguez-Fabià (✉) · L. Johansson · K. Syverud
RISE PFI, Trondheim, Norway
e-mail: sandra.fabia@rise-pfi.no

J. Torstensen
Western Norway University of Applied Sciences, Bergen,
Norway

K. Syverud
Department of Chemical Engineering, NTNU, Trondheim,
Norway

Keywords Cellulose · Hydrophobisation · Plasma etching · Plasma grafting · Adsorption

Introduction

A war is currently raging against the use of fossil fuels, plastic products and plastic waste. Plastic production in 2015 exceeded 380 million tons (Ritchie and Rose 2018). In recent years, more and more attention has been paid to the fact that significant amounts of plastic end up in the ecosystem where it harms living organisms. It has been emphasised in particular that marine ecosystems are vulnerable to nano-/micro- and macroplastic waste (Lamb et al. 2018). According to recent estimates, 11 million tons of plastic end up in the ocean each year (Ocean Conservancy 2021). Macroplastics directly harm organisms by hindering e.g. their movement, while toxic additives and micro-/nanoplastics have a detrimental effect on organisms and cells. Recent studies indicate that current efforts to mitigate plastic waste are insufficient, meaning that the amount of waste will increase, with unpredictable consequences (Borrelle et al. 2020). Finally, the CO₂ emissions associated with plastic production and incineration should not be overlooked (van Heek et al. 2017).

The packaging industry produces by far the most plastic, with output exceeding 140 million tons in 2017 (Ritchie and Rose 2018). Finding alternatives to plastic packaging materials is thus a major focus of current research. Elasticity and hydrophobicity/water repellence are traits inherent in many polymers. These are the main practical advantages of using plastic for packaging. They have also been shown to be the hardest properties to mimic using other materials that have a low carbon footprint and a low likelihood of generating harmful waste. The history of replacing plastic is long and complex. For example, McDonalds recently replaced its plastic straws with cellulose-based straws, which it had used before it began using plastic (Footprint® 2019)! However, paper straws were not as easy to recycle as plastic straws (BBC 2019). Another example is replacing plastic containers with cardboard (e.g. milk cartons). However, such packaging composites typically require a plastic component (Elopak 2021). A mitigating factor in the seemingly “impossible” requirement for a plastic-free packaging material is the changing origin of the polymer, such as Coca Cola’s plant bottle, which has been distributed since 2009 (Ren et al. 2015). Here, the polyethylene terephthalate (PET) is partially made of

wood. The PET monomer can be produced by combining ethylene glycol (EG) with terephthalic acid (TA) (Pang et al. 2016). By producing EG from wood, while the TA is obtained from fossil sources, the plastic resulting from their combination is of about 30% biological origin (Ren et al. 2015). This partially bio-PET may have reduced CO₂ emissions by 315,000 metric tons per year (Ren et al. 2015). Although this makes the plastic partially “non-fossil” in origin, it is clear that it has the same problems in terms of waste generation after use because it is equally difficult to degrade.

Some lignocellulose research focuses on imparting these materials with either the elasticity or the water-resistance of plastic. The best current method for elasticity seems to be single chain dissolution and recasting of cellulose films (Gindl and Keckes 2007) or the aligning of cellulose fibrils (Mohammadi et al. 2017). Such methods typically produce strain at break values of about 10%, whereas values well above 50% are typical for plastic materials. Other options are combining cellulose with smaller amounts of polymer (partial substitution) (Zhao et al. 2018) or seeking inspiration from biological tissue (Wang et al. 2014). However, recent studies indicate that incorporating elastic proteins into nanocellulose films may in fact reduce elasticity (Fang et al. 2017). Currently, it is not yet possible to attain the desired elasticity in lignocellulosic materials.

Hydrophobising lignocellulosic materials may, however, resolve the swelling issues associated with substituting plastic with lignocellulosic materials. Hydrophobisation may be achieved by several methods, including surface modification by polymer grafting or molecular grafting/sorption. This is the first of three reviews addressing hydrophobisation of lignocellulosic materials. The topic of this review is hydrophobisation by physical methods, whereas the second review describes hydrophobisation applying molecular modification and the third review describes hydrophobisation by polymerisation. The three reviews describe hydrophobisation methods for all types of lignocellulosic substrates (i.e. films, fibres, regenerated cellulose fibres, fibrils, crystals, and structures such as membranes) made from all types of raw materials (i.e. wood, bacterial nanocellulose and crops). The aim of these reviews is to present an overview of methods and evaluate them with regards to their

modification process and performance as well as toxicity and food safety.

Lignocellulose chemistry and hydrophobisation

Even if it is well known to the majority of readers of *Cellulose*, a brief summary of lignocellulosic chemistry and structures is given here to provide a complete overview of the substrate to be modified so that it will be fresh in the reader's mind. In addition, the concept of hydrophobicity is explained.

Lignocellulose chemistry and structure

A lignocellulosic material is typically made by refining wood (other sources such as algae, bacteria and tunicates also contain cellulose) in a complex chemo-mechanical process with multiple degrees of freedom (Walker 2006). The resulting lignocellulosic material consists of three biopolymers—cellulose, lignin and hemicellulose—as well as other minor components (Pettersen 1984). The typical content of processed wood is predominantly cellulose, as wood-processing methods often attempt to remove other types of constituents. It should be noted here that both native and refined pulp have a charge from hemicellulose, from sulphonation of lignin or from oxidation of cellulose hydroxyls to carboxylic moieties through the chemical processes applied to isolate cellulose. This charge is typically around 200–300 $\mu\text{mol/g}$ (Ottesen et al. 2017).

Lignocellulosic materials consist of a broad range of materials, such as fibres, sheets and nanocelluloses. Nanocelluloses consist of nanoparticles with at least one dimension below 100 nm and can typically be categorised as either cellulose nanofibrils (CNFs) or cellulose nanocrystals (CNCs). CNFs are isolated

native fibrils or agglomerated native fibrils. They typically have a width of up to 100 nm and a length in the μm -range. CNFs are produced by mechanical deconstruction; often, a mechanical, enzymatic, or chemical pre-treatment, such as 2,2,6,6-tetramethylpiperidin-1-oxyl (TEMPO) mediated oxidation, is utilised to facilitate the fibrillation process. CNCs are shorter, more crystalline types of nanocellulose, with a width between 3 and 50 nm and typical lengths in the range of 50 to 500 nm. CNCs are usually prepared by acid hydrolysis of cotton or purified cellulose. The hydrolysis process introduces functional groups at the surface of the nanocrystals, which depend on the acid used in the reaction. Sulphate and phosphate groups are introduced when H_2SO_4 and H_3PO_4 are used, and hydrolysis with a combination of HCl and an organic acid introduces ester functionalities. Bacterial nanocellulose (BNC) is another type of nanocellulose produced by bacteria of the *Gluconoacetobacter* family. This type of nanocellulose does not contain lignin and is composed of fibrils with diameters under 100 nm, which have very high cellulose purity and low polydispersity in terms of size (Thomas et al. 2018; Tardy et al. 2021).

Cellulose is a linear homopolymer of 1,4-linked β -D-glucopyranosyl units (Fig. 1) (French 2017). In nature, cellulose polymer adopts a planar conformation in which the directly connected glucopyranosyl units are rotated approximately 180° relative to each other (Delmer and Amor 1995). Cellulose is produced by a rosette terminal complex (RTC) enzyme (Atalla and Vander Hart 1999; Kimura et al. 1999). The current view is that chains make fibrils. Both 18 and 24 chain models have been proposed (Cosgrove 2014). The 18-chain model seems to be the most likely configuration (Jarvis 2018). Regardless, single cellulose chains do not exist naturally. This led to the initial belief that cellulose chains are stiff. It is more

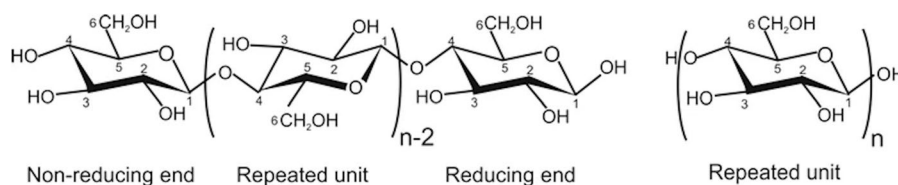


Fig. 1 Cellulose structure. Image obtained from French (2017). Cellulose consists of repeating glucose units (length 0.515 nm) bound through $\beta(1 \rightarrow 4)$ glycosidic bonds (Dufresne

2013). The reducing C1 -OH moiety is in equilibrium with the open ring aldehyde form, and the C4 -OH is the non-reducing end

likely, however, that cellulose chains are comparable to “regular” carbon–carbon linked polymers, as discussed by Bao et al. (2014). Fibrils are stiffer and have been compared to Kevlar fibres (Osong et al. 2016). This is due to both hydrophilic (hydrogen-bonding) and hydrophobic chain interactions. Due to the bundle-like nature of cellulose, determining the degree of polymerisation is inherently difficult. However, it is assumed to range from around 2000 to 20,000 glucose units (Delmer and Amor 1995).

Cellulose has several allomorphs, including I β and I α , which are found in plants. I β is dominant in plants, whereas I α is dominant in algae and bacteria (Delmer and Amor 1995; Atalla and Van der Hart 1999). Cellulose chains bind through two types of interactions. Hydrophilic in-plane interactions (hydrogen bonds) have been carefully examined by Nishiyama et al. (2002, 2003) for the cellulose I β and I α structures. Hydrophobic interplane interactions (van der Waals forces) have been subject to some debate, for example by Lindman et al. (2010), who simply state that hydrophobic interactions are typically neglected between cellulose chains (although they should not be) and that cellulose is inherently amphiphilic. The hydrophobic nature of cellulose has been demonstrated by Staudinger et al. (1953) and Yamane et al. (2006). Yamane et al. (2006) were able to tune the cellulose contact angle (CA) between approximately 10° and 35° by altering the extent to which hydroxyl groups were exposed on the surface.

Lignocellulosic material hydrophobicity and water response

An exact definition of hydrophobicity is discussed by Chandler (2002) and Lum et al. (1999). One way to classify hydrophobicity is as a trait whereby molecules prefer to bind with other non-polar molecules. Likewise, a hydrophilic molecule preferentially binds with another polar molecule. A molecule may be classified as being predominantly polar or non-polar or as being amphiphilic: both polar and non-polar at the same time. As discussed in the previous section, cellulose is amphiphilic. Several methods can be used to quantify molecular polarity, such as the molecular dipole moment (Gubskaya and Kusalik 2002) or interactions with other molecules, such as the Flory χ -parameter (Fox Jr. and Flory 1950).

A common way of characterising a material’s water uptake is determining its ab- or adsorption of water. It has been well established in the lignocellulose field that the surface of a lignocellulosic material—unlike, say, a metal—cannot feasibly be defined. The term “sorption” thus includes both adsorption and absorption of such material and will be used for the remainder of this paper. Lignocellulosic materials are hygroscopic, meaning that they sorb water at ambient conditions and are thus innately hydrophilic. Moreover, they display a water sorption hysteresis (Wahba and Nashed 1957). This means that the water sorption (amount, kinetics) depends on the previous sorption “history” of the materials (i.e. previous contact with water).

Contact angle

The contact angle (θ) is the angle of contact between a droplet and its contacting surface (Fig. 2). A droplet–surface contact angle below 90° is considered hydrophilic, while such an angle above 90° is hydrophobic. Droplet–surface energy can be described according to Young’s Eq. (1):

$$\gamma_{SG} = \gamma_{SL} + \gamma_{LG} \cos(\theta) \quad (1)$$

where θ is the wetting angle, γ_{SL} is the surface–liquid surface energy, γ_{SG} is the solid–gas surface energy, and γ_{LG} is the liquid–gas surface energy (Young 1805; White 1977; Ross and Becher 1992). There are three common ways of reporting the contact angle: by static, receding or advancing CA (Fig. 2). The static contact angle is the angle at which the droplet forms and the contact area is stable over time, i.e. the angle of a fixed volume droplet deposited on a surface where no sorption or evaporation occurs. The dynamic contact angles are measured while the droplet is not in equilibrium. When more liquid is added to the droplet, the advancing CA is measured. When liquid is removed, the receding CA is detected. The receding CA is always smaller than the advancing CA, and the difference between the two is referred to as the contact angle hysteresis (Gao and McCarthy 2006).

The contact angle may be affected by surface structure or chemistry. For example, hydrophilic agar gels display contact angles of approximately 20°, and PTFE (Teflon, polytetrafluorethylene) has a CA of

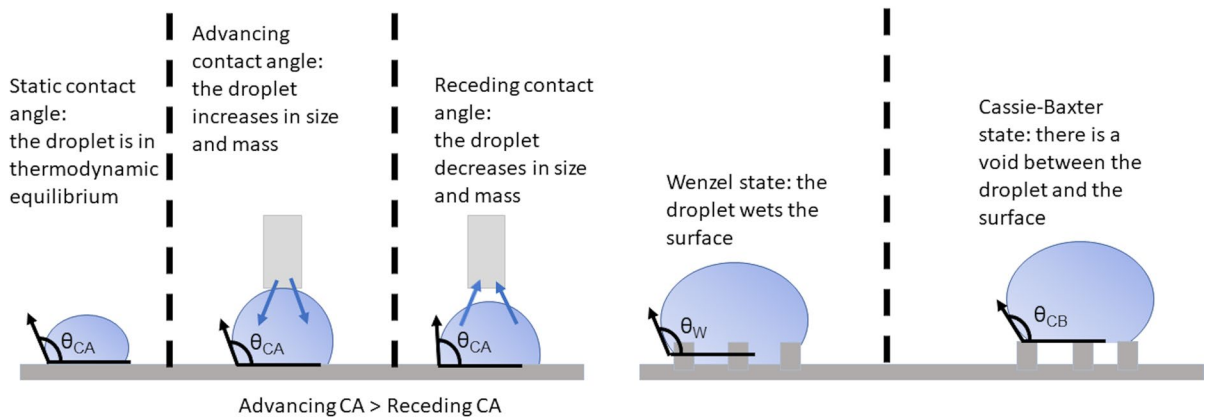


Fig. 2 Illustration of the contact angle and different wetting states. θ_{CA} : contact angle, θ_W : Wenzel-state angle, θ_{CB} : Cassie-Baxter state angle

approximately 90° – 100° (Yasuda et al. 1994). These differences in contact angle may be directly related to the hydrophobic and hydrophilic chemical nature of the material. Agar is a hydrophilic saccharide-polymer, with hydroxyl moieties along the chain. Teflon has fluor-substituted carbon atoms as the repeating unit and is commonly used to obtain water-repellent surfaces.

Roughness and surface nanostructuring may be used to create both hydrophilic and hydrophobic surfaces. Typically, surfaces with high roughness in the micro- and nanoscale tend to be more hydrophobic due to a decrease in the droplet/surface contact area (Wenzel 1936; Feng et al. 2002). Thus, smoother surfaces of the same material are more hydrophilic.

Lignocellulosic materials sorb water due to their porous structures and highly hydrophilic surfaces. Thus, the contact angle is time dependent and always dynamic (Dankovich and Gray 2011). For the same reason, the contact angle also decreases with increasing relative humidity. This is due to enhanced sorption of water at higher humidities and thus a hydrophilisation of the material (Hammes et al. 2016). For this reason it is difficult to detect the contact angle of these materials, especially when also factoring for the surface having an inherent surface structure, e.g. roughness. The contact angle of lignocellulosic materials is often reported to be between 20° and 50° (Atalla et al. 1980; Fortunati et al. 2012; Nagalakshmaiah et al. 2016b); however, values down to 8.6° have been reported (Abitbol et al. 2014). This should be related to the work described earlier by Yamane

et al. (2006) indicating that the contact angle depends on the orientation of cellulose chains.

In this context, it is worth emphasising that the chemical composition of lignocellulosic materials influences the contact angle. For example, Spence et al. (2010) investigated the impact of lignin on the contact angle. They demonstrated a correlation between the lignin content of the samples and the contact angle in which pulp samples with higher lignin content presented higher contact angles. For instance, thermomechanical pulp (31.2% lignin content) presented a contact angle of 80° , whereas bleached softwood (0.8% lignin content) presented a contact angle of 20° . The same correlation was observed for microfibrillated cellulose film prepared from the same pulp. This should be related to the more hydrophobic lignin structure. Another alternative is the hot-pressing of lignocellulosic pulp. In a very instructive paper, Joelsson et al. (2020) showed that the contact angle of sheets made from hot-pressed pulp could be increased and, in some cases, reach values above 90° . This was attributed to the resulting higher material density after pressing, as well as the lignin content and the type of lignin. It should be noted that some pulps never achieved CAs $> 90^\circ$, and that water droplets on these sheets would, as expected, be sorbed by the material over time.

The contact angle has been used to characterise lignocellulosic materials with regard to packaging (Spence et al. 2010; Rodionova et al. 2011) and oil/water separation applications (Arslan et al. 2016). In other applications, contact angle measurements have

been used to characterise nanocellulose composite films used for food packaging (Slavutsky and Bertuzzi 2014).

Superhydrophobicity

As discussed, a hydrophobic surface is defined as a material that gives a $CA > 90^\circ$. Another distinction is commonly made between hydrophobicity and superhydrophobicity, wherein superhydrophobicity is given by a $CA > 150^\circ$. Superhydrophobicity may be achieved by increasing the surface roughness (Whyman et al. 2008). This modification is typically expressed by the Wenzel equation (2, Fig. 2):

$$\cos(\theta_w) = r \cdot \cos(\theta_s) \quad (2)$$

where θ_w is the Wenzel contact angle, θ_s is the contact angle of the smooth surface and r is the increase in solid-liquid interfacial area due to roughness compared to a smooth surface (Wolansky and Marmur 1999). Another possibility is that there are voids between the droplet and the surface. In these cases, the Cassie-Baxter equation (Whyman et al. 2008; Milne and Amirfazli 2012) (3, Fig. 2) states that:

$$\cos(\theta_{CB}) = f \cdot \cos(\theta_s) - (1 - f) \quad (3)$$

where θ_{CB} is the Cassie-Baxter contact angle, f is the fraction of solid surface area in contact with the droplet and $1-f$ is the fraction of voids. For practical applications of the Cassie-Baxter or Wenzel equations in surface design, the reader is referred to works by e. g. Zhao et al. (2014).

Physical hydrophobisation techniques

There are many different approaches to physically modifying cellulosic substrates in order to achieve hydrophobic properties. In this review, we will focus on the techniques of adsorption and plasma.

Adsorption

Adsorption has been used to modify the surface of (nano)celluloses. This process relies on physical interactions between the adsorbed molecule and the cellulosic substrate, such as affinity between hydrophilic groups, the surface structure, electrostatic interactions, hydrogen bond formation or van der Waals interactions (Rechendorff et al. 2006; Habibi 2014; Hubbe et al. 2015). The process of adsorption is illustrated in Fig. 3.

Surfactants

Surfactants are amphiphilic molecules with a hydrophilic head and a polar tail and can be classified according to the charge of the hydrophilic domain as anionic, cationic and non-ionic surfactants. Anionic surfactants are used the most for the modification of cellulosic materials, followed by non-ionic and cationic surfactants (Tardy et al. 2017). Modifications by surfactant adsorption are summarised in Table 1.

By the 1930s, the adsorption of surfactants onto cotton and wool was already the subject of interest. In Adam's studies (1937), he reported detergent adsorption onto wool and cotton. For cotton, the adsorption of all detergents was quite similar, with cetane sodium sulphonate displaying the highest adsorption. Meader and Fries (1952) investigated the adsorption of two anionic surfactants, namely sodium alkyl aryl sulphonate and sodium palmitate, on cotton and wool cloth in the presence of salts and in hard and distilled water. The addition of salts increased the adsorption of alkyl aryl sulphonate, while the adsorption of sodium palmitate remained unchanged.

Simončič and Rozman (2007) investigated the effects of three different surfactants on desized fabric and alkaline-scoured woven cotton fabric. The chosen surfactants were two anionic surfactants—sodium dodecyl sulphate (SDS) and sodium dioctyl sulfosuccinate (SDOSS)—and the non-ionic

Fig. 3 Schematic representation of the adsorption process where the adsorbent is deposited on the material surface

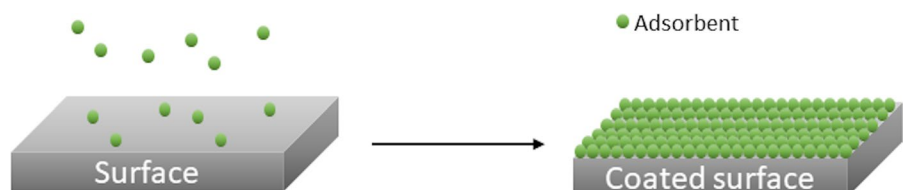


Table 1 Overview of surface modifications of cellulosic materials by surfactant adsorption

Source of cellulose	Type of cellulose	Surfactant	Contact angle (°)	References
Cotton fabric	Cotton	Soap, cetyl sodium sulphate, Lissapol AT, cetane sodium sulphate, Igepon T, amide-based detergent	–	Adam (1937)
Cotton fabric	Cotton	Sodium alkyl aryl sulphate, sodium palmitate	–	Meader and Fries (1952)
Cotton fabric	Desized woven cotton fabric (D), alkaline-scoured woven cotton fabric (A)	SDS, SDOSS, Triton X 100	SDS: D=88.9, A=84.0 SDOSS: D=89.4, A=81.7 Triton X 100: D=89.0, A=81.1*	Simončič and Rozman (2007)
Cotton, tunicate, MCC	CNC	PEPNP	–	Heux et al. (2000), Bonini et al. (2002), Ljungberg et al. (2005), Elazzouzi-Hafraoui et al. (2009), Fortunati et al. (2012)
MCC	CNC	STEFAC TM 8170	–	Arrieta et al. (2014a, b)
MCC from Norway spruce	CNW	PEPNP	–	Bondeson and Oksman (2007)
Whatman cotton filter paper	CNC	CTAB	27	Abitbol et al. (2014)
	CNC	CTAB	45	Nagalakshmaiah et al. (2016a)
Never-dried softwood sulphite pulp	TEMPO-oxidised CNC	Quaternary ammonium salts	71	Salajková et al. (2012)
Bleached softwood kraft pulp	TOCNF	CTAB, DDDAB	CTAB: ≤ 71.7 DDDAB: ≤ 67.7	Xhanari et al. (2011)
Bleached softwood kraft pulp	TOCNF	CTAB	33.1	Qu et al. (2019)

*The maximum advancing contact angle values obtained with these surfactants are presented. The surfactant concentration varies in each case

surfactant Triton X 100 (4-(1,1,3,3-tetramethylbutyl) phenyl polyoxyethylene(10)-ol). The desized fabric presented hydrophobic properties, whereas the alkaline-scoured fabric was hydrophilic. The presence of surfactants increased the wettability of the apolar desized sample. The surfactants were adsorbed with the hydrophobic tail towards the cotton surface and the hydrophilic group towards water. The alkaline-scoured fabric, on the other hand, had a polar surface in which, at low surfactant concentrations, the molecules adsorbed with the polar headgroup towards the cotton surface and the hydrophobic tail towards water, with the surface thus becoming more hydrophobic. At

high surfactant concentrations, the molecules self-assembled into bilayers, rendering the surfaces hydrophilic again.

Heux et al. (2000), Bonini et al. (2002) and Elazzouzi-Hafraoui et al. (2009) were the first to describe the use of surfactants to stabilise cellulose nanocrystals in nonpolar solvents. They used a commercial phosphoric ester of polyoxyethylene (9) nonylphenyl ether (PEPNP) surfactant to disperse cotton and tunicate CNCs in toluene and cyclohexane. The adsorbed anionic surfactant-to-cellulose weight ratio was 0.7 for cotton and 1.5 for tunicate (Heux et al. 2000). In a later publication, Ljungberg et al. (2005) followed

the same procedure to disperse CNCs in an atactic polypropylene matrix. The nanocomposite films containing surfactant-dispersed crystals displayed better mechanical properties than did films with aggregated and grafted CNCs. PEPNP and STEFAC TM 8170, a commercial surfactant of nonylphenol polyoxyethylene (10) phosphate ester, were used to disperse CNCs in poly(lactic acid) (PLA) and poly(lactic acid)-poly(hydroxybutyrate) (PLA-PHB) matrices. The results showed an improvement in the nanoparticle/polymer adhesion and enhanced blending between PLA and PHB, as well as reduced water vapour permeability and oxygen transmission (Fortunati et al. 2012; Arrieta et al. 2014a, b). However, Bondeson and Oksman (2007) showed that the surfactant (phosphoric ester of PNEP) used in cellulose nanowhiskers (CNW)/PLA composites contributed to the degradation of PLA.

Cationic surfactants containing ammonium bromide moieties have been widely used for hydrophobisation of cellulosic materials. The adsorption of cetyltrimethylammonium bromide (CTAB) onto CNCs has increased the contact angle of CNC film from 8.6° to 27° (Abitbol et al. 2014). It was possible to tune the charge coupling efficiency between the surfactant and the CNCs by varying the reaction conditions. Polypropylene nanocomposites were prepared using modified CNCs as nanofillers (Nagalakshmaiah et al. 2016a). CTAB was adsorbed onto the CNCs, which were successfully dispersed in toluene, ethyl acetate and chloroform. Sheet samples of modified CNCs presented a higher contact angle (45°) than the unmodified CNCs (24°) and showed improved thermal stability. The polypropylene nanocomposites reinforced with CNCs and modified CNCs displayed an improvement of the elongation at break compared to pure polypropylene. Quaternary ammonium salts have also been used to

modify the surface of CNCs from TEMPO-oxidised pulp (Salajková et al. 2012). After adsorption of four different surfactants with long alkyl, phenyl, glycidyl and diallyl groups, the surfaces became more hydrophobic, allowing the dispersion of the CNCs in chloroform and toluene. A model surface was prepared by coating CNCs with a C18 alkyl chain ammonium salt. The water contact angle increased from 12° to 71° . The density of adsorbed surfactant molecules can be tuned by varying the number of carboxylic acids of the TEMPO-oxidised pulp.

Xhanari et al. (2011) investigated the adsorption of the cationic surfactants CTAB, dihexadecyldimethylammonium bromide (DHDAB) and didodecyldimethylammonium bromide (DDDAB) onto TEMPO-oxidised CNFs (TOCNFs) with varying charge densities. Adsorption of surfactants was favoured in samples with a higher charge density. At low surfactant concentrations, the fibrils became more hydrophobic, but above a certain concentration, the surfactant molecules formed bilayers with the hydrophilic groups in contact with the water phase, increasing the hydrophilicity of the fibrils. In addition, the adsorption of double chain surfactants was slightly higher due to the more efficient packing of the molecules. Similarly, CTAB was used for the hydrophobisation of TOCNFs and, as a consequence, deconstructed the gel structure (Qu et al. 2019). A schematic representation of the process is shown in Fig. 4. A quantity of 2.16 mmol CTAB/g TOCNFs was required to achieve approximately 100% charge coupling. The viscosity of the hydrogels decreased with increasing CTAB concentration due to a decrease in the interactions between the carboxyl and hydroxyl groups, and the water contact angle of films prepared from modified and unmodified TOCNFs increased from 15.7° to a maximum of 33.1° respectively.

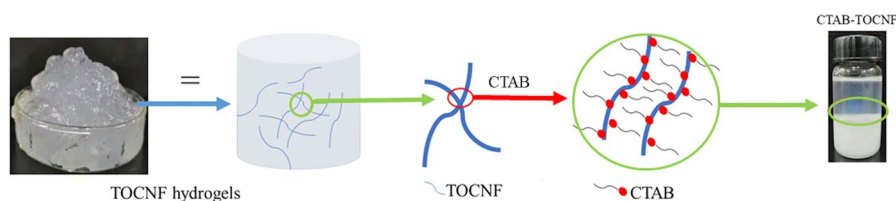


Fig. 4 Example of TEMPO-oxidised CNFs (TOCNFs) modified by surfactant adsorption. The figure shows a schematic representation of TOCNFs forming a gel structure, followed by a zoom of two CNFs. The addition of cetyltrimethylammonium

bromide (CTAB) results in adsorption of the surfactant on the CNFs and the separation of the CNFs and deconstruction of the gel into a two-phase system. Image adapted from Qu et al. (2019)

For more detailed information on surfactant adsorption onto cellulosic materials, the reader is referred to a review by Tardy et al. (2017).

Waxes

Waxes can have diverse origins and are classified accordingly. Natural waxes, from both animal and vegetal sources, are lipids that contain complex mixtures of compounds such as hydrocarbons, fatty acids, fatty alcohols, wax esters, ketones and sterols (Doan et al. 2017). Waxes can also be of mineral origin (petroleum, coal and peat) or synthetic origin through polymerisation of feed stocks (Leray 2007).

Wax-coated CNF films were prepared by pressurized filtration by Österberg et al. (2013). The films presented resistance to several solvents, such as water, methanol, toluene, and dimethylacetamide. Some of the films were coated by dipping them into melted wax. The increased contact angle of the coated film (from 40° to 110°) showed that the surfaces had become more hydrophobic. The oxygen and water vapour barrier properties of the films were improved upon coating. Korhonen et al. (2020) prepared hydrophobic all-cellulose composites using cationic starch and carnauba wax (CW). Kraft fibres were dispersed in pulp dissolved in NaOH. The dried composite was first dipped into a starch solution, then dipped into a CW dispersion until two bilayers were obtained. Samples that were dried after layer-by-layer deposition of the coatings achieved contact angles between 88° and 104°, while samples that underwent a double-drying procedure achieved contact angles between 100° and 122°. Although the secondary drying increased the contact angle of the substrates, it had a detrimental effect on the mechanical properties of the samples. Therefore, the coating system was optimised by way of spraying, which resulted in contact angles of 110° (one bilayer) and 120° (two bilayers) while maintaining the mechanical properties of the substrates.

Beeswax (BW) is a food-grade wax that is of interest in food-packaging applications. Indriyati et al. (2020) prepared bacterial nanocellulose films containing up to 40% BW for this purpose. The films contained carboxymethyl cellulose (CMC), which was added as homogeniser, and the surfactant Tween 80. The contact angle of the BNC films was 45°, and the BNC/CMC films had a contact angle of 53°. Addition of 40 wt% BW resulted in film with

contact angles of 124°. Hutton-Prager et al. (2021) impregnated paper samples with vegetable wax (VW) and a mixture of beeswax and carnauba wax. The authors investigated the effect of the annealing temperature on the hydrophobicity of the samples. Annealing both types of samples at 140 °C resulted in contact angles between 110° and 120°, while annealing at 160 °C resulted in contact angles of 130°. The increase in contact angles was caused by the increased roughness in the micro- and nano-scale that was formed during annealing.

Wang and Zhao (2021) prepared superhydrophobic coatings for food packaging purposes. Filter paper was first sprayed with a beeswax and candlelilla wax emulsion. Spraying emulsions on it with a concentration of 10 mg wax/ml yielded superhydrophobic surfaces for both types of waxes. Double-layer coatings were prepared by coating the paper first with either zein/pectin (ZP) particles with CNF or precipitated calcium carbonate (PCC) particles with CNF and then spraying it with wax emulsion. In all cases, contact angles above 150° were obtained both at room temperature and after cold treatment. After thermal treatment, only the coatings with PCC/CNF achieved superhydrophobicity, although in all cases the substrates became hydrophobic. Honey, milk, coke and tea were also tested on PCC/CNF-coated substrates sprayed with wax, and with the exception of milk, the liquids had contact angles above 150° on all substrates. Milk presented contact angles above 150° only on thermally treated substrates, although in cold-treated or non-conditioned substrates the contact angles of milk were higher than 90°.

Zhang et al. (2014) fabricated superhydrophobic paper using mixtures of carnauba wax and beeswax. Emulsions of BW: CW were prepared at three different weight ratios (7:3, 5:5 and 3:7) and used to coat the surface of copy paper. The samples were annealed at various temperatures and contact angles between 130° and 167° were obtained. The results showed that coating with 70% CW: 30% BW resulted in lower contact angles. This coating method is claimed to be a cost-effective and environmentally friendly approach that yields superhydrophobic surfaces that maintain their properties over six months at atmospheric conditions. An overview of the hydrophobisation approaches using waxes is given in Table 2.

Table 2 Overview of surface modifications of cellulosic materials by wax adsorption

Source of cellulose	Type of cellulose	Wax type	Contact angle (°)	References
Never-dried industrial bleached hardwood kraft pulp	CNF	Paraffin wax	110	Österberg et al. (2013)
Birch dissolving pulp and softwood kraft pulp	Fibre, CNF	CW	Single drying: 88–104 Double drying: 100–122 Spraying: 110, 120	Korhonen et al. (2020)
BNC		BW	45–124	Indriyati et al. (2020)
Whatman filter paper	Fibre	VW BW/CW	140 °C: 110–120 160 °C: 130	Hutton-Prager et al. (2021)
Whatman filter paper	Fibre	BW or candelilla wax + ZP/CNF	> 150	Wang and Zhao (2021)
Whatman filter paper	Fibre	BW or candelilla wax + PCC/CNF	> 150	Wang and Zhao (2021)
Copy paper	Fibre	BW/CW	70% BW: 130–164 50% BW: 153–167 30% BW: 140–159	Zhang et al. (2014)

Lignin

Hydrophobisation of predominantly cellulosic materials (fibres, sheets and nanocelluloses) may also be achieved by lignin. A comprehensive review of lignin-containing cellulose nanomaterials was recently carried out by Liu et al. (2021). Uses for lignin containing nanocellulose include, among others, composite reinforcement, emulsion stabilisation, paper manufacturing and electronics. Lignin-based coatings have been used to increase the hydrophobicity of substrates, but in some cases the lignin present in the raw materials has been sufficient to obtain

substrates with enhanced hydrophobicity. Some of these examples are shown below and summarised in Table 3.

Lignin has a contact angle of 30°–60° (Notley and Norgren 2010; Wei et al. 2018) and is thus more hydrophobic than cellulose. Kraft pulp fibres (eucalyptus) also demonstrated a reduction in the water retention value, dropping, for example, from 88 to 64% when the lignin content was increased from 3.9 to 17.2% (Bian et al. 2017). Hua et al. (2019) prepared hydrophobic lignin derivatives by way of esterification with oleic acid. A suspension of esterified lignin was sprayed and spin-coated onto bleached

Table 3 Overview of hydrophobisation of cellulosic materials with lignin

Source of cellulose	Type of cellulose	Wax type	Contact angle (°)	References
Kraft pulp sheets	Fibre	Softwood kraft lignin esterified with oleic acid	Spraying: 123 Spin-coating: 122	Hua et al. (2019)
Wood (yellow poplar)			Spraying: 147 Spin-coating: 137	
Paperboard	Fibre	Softwood kraft lignin esterified with TOFA	80	Hult et al. (2013)
Munktell filter paper	Fibre	Softwood kraft lignin	Not measurable (after 10 min.)	Antonsson et al. (2008)
Munktell filter paper	Fibre	Softwood kraft lignin reacted with linseed oil	120 (after 10 min.)	Antonsson et al. (2008)
Munktell filter paper	Fibre	Linseed oil	120 (after 10 min.)	Antonsson et al. (2008)
Moso bamboo (fibre (F) and parenchyma cells (P))	CNF	–	F: 72.4 P: 66.5	Zhang et al. (2020)

kraft pulp sheets and wood. The contact angle of the pulp sheets increased from 80° to 122° – 123° with both coating approaches, and the contact angle of the wood (68°) increased to 147° by way of spraying and to 137° by way of spin-coating. Similarly, Hult et al. (2013) prepared lignin esterified with a tall oil fatty acid (TOFA) and used it to coat paperboard samples. The samples coated with the lignin derivative presented a contact angle of 80° which was stable for two minutes, whereas the paperboard coated with only the fatty acid (TOFA) presented a decrease in contact angle over time. However, the contact angle over time of the lignin-TOFA-coated samples was only marginally higher than that of the uncoated paperboard. The water vapour and oxygen transmission rates of paperboard were decreased by the lignin-TOFA coating, although even lower values were obtained with the TOFA coating. Antonsson et al. (2008) modified lignin with linseed oil. Filter paper was coated with lignin, the lignin derivative and pure linseed oil. After 10 min, the samples coated with the lignin derivative and linseed oil presented a contact angle of 120° , whereas the water droplet had been absorbed by the lignin-coated sample. The lignin derivative and linseed oil were added to mechanical pulp prior to the formation of sheets. The lignin derivative presented homogeneous distribution and good affinity with the pulp fibres, in contrast to the linseed oil.

Considering that lignin is not hydrophobic ($CA < 90^\circ$), it may be used as a (nano)cellulose compatibiliser in (nano)composites. One such example is the lignin-enrichment of CNCs to enhance particle dispersibility in polylactic acid (PLA, with $CA = 88^\circ$ – 89°) (Wei et al. 2018). CNCs with high lignin content can be obtained by way of lignin coating (BLCNCs) or by producing CNCs that contain more lignin that is not necessarily located at the surface (HLCNCs). HLCNCs contained 46% more lignin than BLCNCs. PLA composites containing HLCNCs present lower adhesion factors than composites with BLCNCs, which is an indication of enhanced compatibility of the HLCNCs and the PLA matrix. The addition of HLCNCs improves the material toughness and thermal stability to a greater extent than does the addition of BLCNCs. In another work by Zhang et al. (2020), lignocellulose nanofibrils (LCNFs) were used to make films. The LCNF films displayed higher contact angles (66° – 72°) than the CNF films (24° – 26°), and LCNF films also had reduced stress at break (184

vs 160 MPa). The reduction in strength was attributed to the disruption of cellulose hydrogen bonds.

Plasma-induced modifications

Plasma is used to physically and chemically modify surfaces. The ionised molecules present in the plasma state can increase *the surface roughness* by etching and/or *activating the surfaces*, enabling the grafting of molecules. Both etching and activation can modify the properties of the surfaces only and can be used to increase the hydrophobicity of the substrates. Plasma technology is regarded as environmentally friendly because it does not require the use of solvents. Nevertheless, fluorinated species are often used as precursors in plasma treatment (Dimitrakellis and Gogolides 2018). Modifications by plasma are summarised in Table 4.

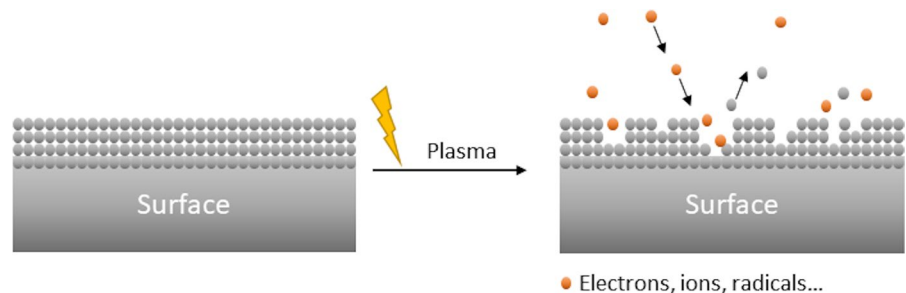
Plasma etching

Plasma etching is a useful and inexpensive technique for obtaining (super)hydrophobic surfaces. Etching increases the roughness of the substrates and is typically followed by coating with a hydrophobic compound (Dimitrakellis and Gogolides 2018). In the etching process, the species in the plasma (ions, radicals and electrons) collide with the surface, resulting in the sputtering of atoms (Nageswaran et al. 2019). This process is depicted in Fig. 5.

Superhydrophobic paper was prepared using a combination of plasma etching and plasma deposition of octafluorocyclobutane ($c\text{-C}_4\text{F}_8$) (Dimitrakellis et al. 2017). Atmospheric pressure He/O₂ plasma selectively removed the top cellulose fibres, forming a hierarchical topography of the surface. The fluorocarbon coating was used to modify the surface energy of the paper samples. Various types of paper (blank and colour-printed copy-grade paper and paper from an old printed document) were treated following this procedure. In all cases, superhydrophobicity was achieved, with contact angles between 158° and 160° . Longer etching treatments combined with fluorocarbon deposition resulted in oleophobic surfaces. Etching and coating with fluorocarbon (pentafluoroethane) were also used to obtain superhydrophobic copy paper and handsheets (Balu et al. 2008). Both substrates presented contact angles of around 165° . In this approach, oxygen plasma etching was

Table 4 Overview of modifications of cellulosic materials by radiation-induced modification

Plasma etching					
Cellulose source	Type of cellulose	Reagent	Contact angle (°)	References	
Paper	Fibre	c-C ₄ F ₈	158–160	Dimitrakellis et al. (2017)	
Copy paper	Fibre	Pentafluoroethane	ca.166	Balu et al. (2008)	
Handsheets	Fibre	Pentafluoroethane	166.7	Balu et al. (2008)	
BNC		TCMS	132.6	Leal et al. (2020)	
Plasma grafting					
Cellulose source	Type of cellulose	Monomer	Grafting yield (%)	Contact angle (°)	References
Viscose rayon	Fibre	Dodecyl acrylate		142	Panda et al. (2015)
Viscose rayon	Fibre	Lauryl alcohol		139	Panda et al. (2015)
Viscose rayon	Fibre	Dodecanoic acid		135	Panda et al. (2015)
Viscose rayon	Fibre	Dodecane		139	Panda et al. (2015)
Viscose rayon	Fibre	Propane		97.6	Panda et al. (2015)
Cotton linter	Fibre	TMCS		ca. 150	Lin et al. (2015)
Handsheet paper	Fibre	Vinyltrimethoxysilane		98	Belgacem et al. (2011)
Handsheet paper	Fibre	γ-methacryloxypropyltrimethoxysilane		100	Belgacem et al. (2011)
Handsheet paper	Fibre	β-myrcene		98	Belgacem et al. (2011)
Handsheet paper	Fibre	limonene		112	Belgacem et al. (2011)
Handsheet paper from Kraft pulp	Fibre	CF4		< 120	Sapieha et al. (1990)
Spanish Broom	Fibre	Carbon tetrafluoride		131–148	Tursi et al. (2019)
Unbleached kraft pulp	Fibre	Butyric acid	15		Popescu et al. (2011)
Unbleached kraft pulp	Fibre	Oleic acid	56		Popescu et al. (2011)
Bleached kraft pulp	Fibre	Butyric acid	3		Popescu et al. (2011)
Bleached kraft pulp	Fibre	Oleic acid	9		Popescu et al. (2011)
Spanish Broom	Fibre	Butyric acid	19.3		Totolin et al. (2008)
Spanish Broom	Fibre	Oleic acid	53.6		Totolin et al. (2008)
Spanish Broom	Fibre	Acid mixture from olive oil	45.8		Totolin et al. (2008)

Fig. 5 Schematic representation of the plasma etching process, where the species present in plasma collide with the substrate and sputter atoms from the surface

used to erode the amorphous regions of the cellulose fibres. Surfaces that were coated with pentafluoroethane only became hydrophobic, with contact angles

close to 140°, but only by combining etching and fluorocarbon deposition could superhydrophobicity be attained. Scanning electron microscope (SEM)

images of the untreated and modified handsheet fibres are shown in Fig. 6

Membranes made of bacterial nanocellulose were modified using oxygen plasma treatment followed by vapour deposition of trichloromethylsilane (TCMS) (Leal et al. 2020). The modified membranes presented contact angles of 132.6° . The contact angles remained unchanged after six months of storage in air and decreased to 108° when the membrane was stored in water for a month, demonstrating that the surface modification was highly stable. These modified bacterial nanocellulose membranes were suitable materials for cell culture and microfluidic devices.

Plasma grafting

In plasma, peroxide radicals are formed that initiate radical reactions that graft molecules to the activated surfaces. Often, these chain radical reactions result in the grafting of polymers (Couturand et al. 2015). However, in this review, we will focus on modifications by non-polymeric molecules. Modification by silanes is also included, although they

can polymerise. The principle of plasma grafting is illustrated in Fig. 7. This process consists of three different stages: first, activation of the surface by the abstraction of hydrogen atoms, then the formation of peroxide radicals and, lastly the grafting of the modifying agent.

Helium plasma was used to modify viscose rayon with the precursors dodecyl acrylate, lauryl alcohol, dodecanoic acid and dodecane (Panda et al. 2015). Water contact angles between 135° and 142° were obtained after grafting and washing with solvents. The changes in the contact angles after washing with soap were almost negligible.

Cellulose aerogels prepared from cotton linter were hydrophobised using trimethylchlorosilane as cold plasma (Lin et al. 2015). The aerogels achieved superhydrophobic properties (contact angle of approximately 150°) after three minutes of plasma treatment, and the modification also took place within the aerogel as shown in Fig. 8. The figure shows the sorption of methyl orange aqueous (MOA) and diesel droplets on an unmodified and a modified aerogel. Aerogels can be used as

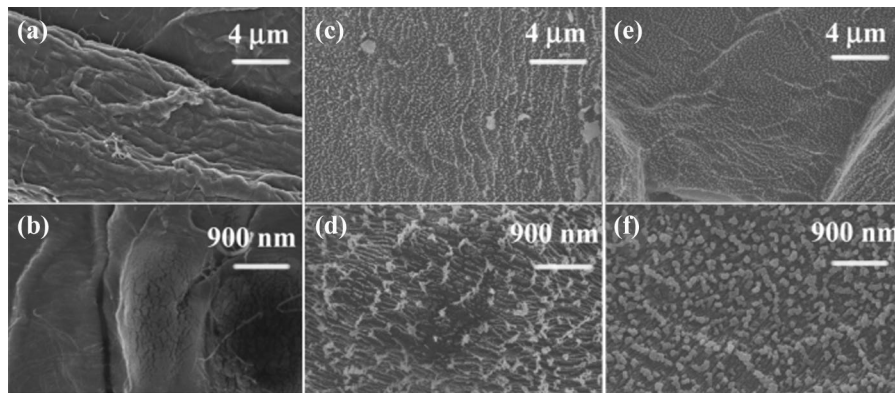


Fig. 6 SEM images of **a, b** untreated handsheet fibres, **c, d** oxygen-etched handsheet fibres and **e, f** oxygen-etched and PFE-coated handsheet fibres. The magnification of the images is $5000\times$ (**a, c, e**) and $20,000\times$ (**b, d, f**). (Reprinted (adapted)

with permission from Balu, B.; Breedveld, V.; Hess, D. W., Fabrication of “Roll-off” and “Sticky” Superhydrophobic Cellulose Surfaces via Plasma Processing. *Langmuir* 2008, 24(9), 4785–4790. Copyright 2008 American Chemical Society

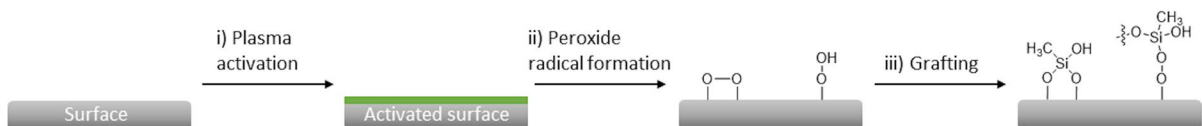
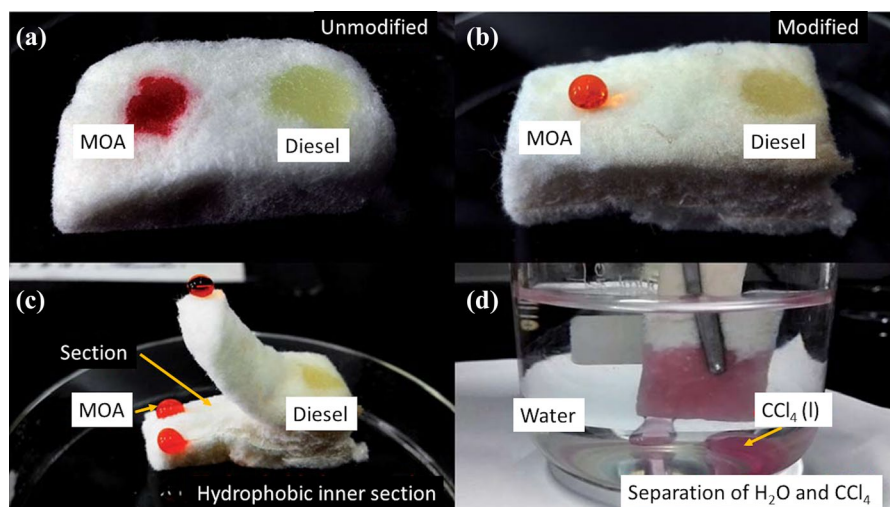


Fig. 7 Schematic representation of the plasma grafting process

Fig. 8 Sorption of methyl orange aqueous (MOA) and diesel droplets on cellulose aerogels from cotton coated with trimethylchlorosilane: **a** unmodified aerogel, **b** modified aerogel, **c** cross-section of the modified aerogel and **d** modified aerogel used to sorb dyed CCl_4 . Image adapted from Lin et al. (2015)



oil adsorbents, with sorption properties that remain constant after 15 cycles.

Handsheet papers modified with silanes (γ -methacryloxypropyltrimethoxysilane, vinyltrimethoxysilane) and natural compounds (β -myrcene, limonene) were prepared and resulted in hydrophobic substrates with contact angles between 98° and 112° (Belgacem et al. 2011). Measurement of the surface energy contributions showed that the modified substrates became nonpolar, with polar surface energy components in the range of 0.2 – 0.8 mJ/m^2 .

Plasma fluorination has also been used as a method for increasing the hydrophobicity of cellulose. Carbon tetrafluoride is typically chosen as the fluorinating agent. Examples of hydrophobisation of handsheet paper (Sapieha et al. 1990) and Spanish Broom fibre (Tursi et al. 2019) with CF_4 show that contact angles can be achieved of up to 120° and 148° respectively.

Cellulose fibre from bleached and unbleached kraft pulp was grafted with butyric and oleic acids (Popescu et al. 2011). Higher degrees of grafting were achieved with the unbleached pulp (15% butyric acid, 56% oleic acid) than with bleached pulp (3% butyric acid, 9% oleic acid). This difference in the grafting might be explained by the presence of lignin in the unbleached pulp, which contributes to the generation of radicals. Similarly, Spanish Broom fibre was modified with butyric acid, oleic acid and a mixture of fatty acids from olive oil (Totolin et al. 2008). All of the fatty acids were successfully grafted, with respective grafting yields of 19.3%, 53.6% and 45.8%.

Discussion

This is the first in a series of three reviews of hydrophobisation of cellulosic materials. Here, examples of modifications achieved by physical methods have been summarised. Perhaps unsurprisingly, adsorption in general yields the lowest contact angles. In all of the examples given in this review of hydrophobisation by surfactant adsorption, the contact angles achieved are below 90° , which is the requirement for a material/surface to be considered hydrophobic. However, in all cases, the hydrophobicity of the substrate has increased compared with its original state. Adsorption of surfactants is primarily used to increase the compatibility/dispersibility of different types of nanocellulose in various solvents, (nano)composites and polymers. In these cases, it has been shown that it is not necessary to achieve hydrophobicity. Decreasing the hydrophilicity of the nanocellulose is sufficient. On the other hand, approaches based on coatings with waxes and lignin-derivatives have yielded surfaces that achieved superhydrophobic properties.

Plasma-treated samples achieve very high contact angles, achieving, in some cases, superhydrophobic properties. These outstanding results are obtained through both etching and grafting. Of the two, plasma etching produces perhaps higher contact angles. As mentioned earlier in this review, plasma technology has many advantages over, for example, chemical modification of cellulose. Plasma is a simple technique that is considered environmentally friendly because it does not require the use of solvents. However, in many of the

examples listed above, compounds containing fluor are used as hydrophobing agents. The use of these chemicals typically yields very high contact angles on the modified substrate. However, compounds containing fluor are harmful to the environment, and efforts should be made to find alternative chemicals and techniques that are more environmentally friendly but provide similar hydrophobicity. Even when comparing these two techniques with chemical modification approaches (see *Hydrophobisation of lignocellulosic materials part II: chemical modification* and *Hydrophobisation of lignocellulosic materials part III: modification with polymers*), adsorption provides the lowest level of hydrophobicity and plasma provides some of the best results.

With regard to the implementation of adsorption and plasma techniques on an industrial scale, simple coating techniques (dip-coating, spraying, roll-coating etc.) are the most common coating approaches due to their simplicity and low cost. The implementation of plasma technology is still limited to certain sectors, such as the textile industry, where plasma has been used for decades. For instance, roll-to-roll low-pressure gas plasma systems are used in the textile industry for surface activation of textiles (Zille et al. 2015). Another growing sector is packaging, particularly food packaging, where plasma, in addition to being used for surface modification, can also provide sterile packaging materials (Pankaj et al. 2014; Zhang 2022). Some types of plasma are more challenging to use on an industrial scale. For instance, vacuum plasma can only be used in batches and requires a vacuum, which is expensive on an industrial scale. Similarly, plasma that requires the use of noble gases can also become costly when used on a large scale (Cvelbar et al. 2019). In order to fully exploit the potential of plasma technology, there is a need to further develop more economical approaches, such as atmospheric pressure plasma technology, and to improve the precision of the plasma technology in order to produce smart surfaces, as well as to improve the coating quality of three-dimensional objects (Cvelbar et al. 2019).

Conclusions

This review is the first in a series of three comprehensive reviews of the hydrophobisation of cellulosic materials. Here, two different physical methods of

modifying cellulosic materials have been described, namely adsorption of molecules and plasma treatment. The two principles are very different and non-comparable, as are the results summarised in this review. While in most cases adsorption of molecules (particularly surfactants) does not increase the hydrophobicity of the materials significantly, super hydrophobic materials are often obtained by plasma-aided modifications.

Acknowledgments The authors would like to acknowledge the Research Council of Norway and its funding of the NanoPlasma project (274975).

Author's contribution Sandra Rodríguez-Fabià: literature search and analysis, writing and revision of the manuscript Jonathan Torstensen: idea for the article, literature search and analysis, writing and revision of the manuscript. Lars Johansson: idea for the article, revision of the manuscript. Kristin Syverud: idea for the article, revision of the manuscript.

Funding Open access funding provided by RISE Research Institutes of Sweden. We gratefully acknowledge the Research Council of Norway and its funding of the NanoPlasma project (274975).

Data availability None.

Declarations

Conflict of interest The authors all declare that there is no conflict of interest.

Open Access This article is licensed under a Creative Commons Attribution 4.0 International License, which permits use, sharing, adaptation, distribution and reproduction in any medium or format, as long as you give appropriate credit to the original author(s) and the source, provide a link to the Creative Commons licence, and indicate if changes were made. The images or other third party material in this article are included in the article's Creative Commons licence, unless indicated otherwise in a credit line to the material. If material is not included in the article's Creative Commons licence and your intended use is not permitted by statutory regulation or exceeds the permitted use, you will need to obtain permission directly from the copyright holder. To view a copy of this licence, visit <http://creativecommons.org/licenses/by/4.0/>.

References

- Abitbol T, Marway H, Cranston Emily D (2014) Surface modification of cellulose nanocrystals with cetyltrimethylammonium bromide. *Nord Pulp Pap Res J* 29(1):46–57. <https://doi.org/10.3183/npprj-2014-29-01-p046-057>

- Adam NK (1937) Detergent action and its relation to wetting and emulsification. *J Soc Dyers Colour* 53(4):121–129. <https://doi.org/10.1111/j.1478-4408.1937.tb01955.x>
- Antonsson S, Henriksson G, Johansson M, Lindström ME (2008) Low Mw-lignin fractions together with vegetable oils as available oligomers for novel paper-coating applications as hydrophobic barrier. *Ind Crops Prod* 27(1):98–103. <https://doi.org/10.1016/j.indcrop.2007.08.006>
- Arrieta MP, Fortunati E, Dominici F, Rayón E, López J, Kenny JM (2014a) Multifunctional PLA-PHB/cellulose nanocrystal films: processing, structural and thermal properties. *Carbohydr Polym* 107:16–24. <https://doi.org/10.1016/j.carbpol.2014.02.044>
- Arrieta MP, Fortunati E, Dominici F, Rayón E, López J, Kenny JM (2014b) PLA-PHB/cellulose based films: mechanical, barrier and disintegration properties. *Polym Degrad Stab* 107:139–149. <https://doi.org/10.1016/j.polymdegradstab.2014.05.010>
- Arslan O, Aytac Z, Uyar T (2016) Superhydrophobic, hybrid, electrospun cellulose acetate nanofibrous mats for oil/water separation by tailored surface modification. *ACS Appl Mater Interfaces* 8(30):19747–19754. <https://doi.org/10.1021/acsami.6b05429>
- Atalla RH, Gast J, Sindorf D, Bartuska V, Maciel G (1980) Carbon-13 NMR spectra of cellulose polymorphs. *J Am Chem Soc* 102(9):3249–3251
- Atalla RH, VanderHart DL (1999) The role of solid state ¹³C NMR spectroscopy in studies of the nature of native celluloses. *Solid State Nucl Magn Reson* 15(1):1–19. [https://doi.org/10.1016/S0926-2040\(99\)00042-9](https://doi.org/10.1016/S0926-2040(99)00042-9)
- Balu B, Breedveld V, Hess DW (2008) Fabrication of “roll-off” and “sticky” superhydrophobic cellulose surfaces via plasma processing. *Langmuir* 24(9):4785–4790. <https://doi.org/10.1021/la703766c>
- Bao Y, Qian H-J, Lu Z-Y, Cui S (2014) The unexpected flexibility of natural cellulose at a single-chain level and its implications to the design of nano materials. *Nanoscale* 6(22):13421–13424. <https://doi.org/10.1039/C4NR04862H>
- BBC (2019) McDonald’s paper straws cannot be recycled. <https://www.bbc.com/news/business-49234054>. Accessed 04 Feb 2021
- Belgacem MN, Salon-Brochier MC, Krouit M, Bras J (2011) Recent advances in surface chemical modification of cellulose fibres. *J Adhes Sci Technol* 25(6–7):661–684. <https://doi.org/10.1163/016942410X525867>
- Bian H, Chen L, Dai H, Zhu JY (2017) Integrated production of lignin containing cellulose nanocrystals (LCNC) and nanofibrils (LCNF) using an easily recyclable di-carboxylic acid. *Carbohydr Polym* 167:167–176. <https://doi.org/10.1016/j.carbpol.2017.03.050>
- Bondeson D, Oksman K (2007) Dispersion and characteristics of surfactant modified cellulose whiskers nanocomposites. *Compos Interfaces* 14(7–9):617–630. <https://doi.org/10.1163/156855407782106519>
- Bonini C, Heux L, Cavallé J-Y, Lindner P, Dewhurst C, Terch P (2002) Rodlike cellulose whiskers coated with surfactant: a small-angle neutron scattering characterization. *Langmuir* 18(8):3311–3314. <https://doi.org/10.1021/la015511t>
- Borrelle SB, Ringma J, Law KL, Monnahan CC, Lebreton L, McGivern A, Murphy E, Jambeck J, Leonard GH, Hilleary MA, Eriksen M, Possingham HP, De Frond H, Gerber LR, Polidoro B, Tahir A, Bernard M, Mallos N, Barnes M, Rochman CM (2020) Predicted growth in plastic waste exceeds efforts to mitigate plastic pollution. *Science* 369(6510):1515–1518. <https://doi.org/10.1126/science.aba3656>
- Chandler D (2002) Hydrophobicity: two faces of water. *Nature* 417(6888):491–491. <https://doi.org/10.1038/417491a>
- Cosgrove DJ (2014) Re-constructing our models of cellulose and primary cell wall assembly. *Curr Opin Plant Biol* 22:122–131. <https://doi.org/10.1016/j.pbi.2014.11.001>
- Couturaud B, Baldo A, Mas A, Robin JJ (2015) Improvement of the interfacial compatibility between cellulose and poly(l-lactide) films by plasma-induced grafting of l-lactide: the evaluation of the adhesive properties using a peel test. *J Colloid Interface Sci* 448:427–436. <https://doi.org/10.1016/j.jcis.2015.02.035>
- Cvelbar U, Walsh JL, Černák M, de Vries HW, Reuter S, Belmonte T, Corbella C, Miron C, Hojnik N, Jurov A, Puliyalil H, Gorjanc M, Portal S, Laurita R, Colombo V, Schäfer J, Nikiforov A, Modic M, Kylian O, Polak M, Labay C, Canal JM, Canal C, Gherardi M, Bazaka K, Sonar P, Ostrikov KK, Cameron D, Thomas S, Weltmann K-D (2019) White paper on the future of plasma science and technology in plastics and textiles. *Plasma Processes Polym* 16(1): 1700228 1–37. doi:<https://doi.org/10.1002/ppap.201700228>
- Dankovich TA, Gray DG (2011) Contact angle measurements on smooth nanocrystalline cellulose (I) thin films. *J Adhes Sci Technol* 25(6–7):699–708. <https://doi.org/10.1163/016942410X525885>
- Delmer DP, Amor Y (1995) Cellulose biosynthesis. *Plant Cell* 7(7):987–1000. <https://doi.org/10.1105/tpc.7.7.987>
- Dimitrakellis P, Gogolides E (2018) Hydrophobic and superhydrophobic surfaces fabricated using atmospheric pressure cold plasma technology: a review. *Adv Coll Interface Sci* 254:1–21. <https://doi.org/10.1016/j.cis.2018.03.009>
- Dimitrakellis P, Travlos A, Psycharis VP, Gogolides E (2017) Superhydrophobic paper by facile and fast atmospheric pressure plasma etching. *Plasma Process Polym* 14(3):1600069 1–8. doi:<https://doi.org/10.1002/ppap.201600069>
- Doan CD, To CM, De Vrieze M, Lynen F, Danthine S, Brown A, Dewettinck K, Patel AR (2017) Chemical profiling of the major components in natural waxes to elucidate their role in liquid oil structuring. *Food Chem* 214:717–725. <https://doi.org/10.1016/j.foodchem.2016.07.123>
- Dufresne A (2013) Nanocellulose: from nature to high performance tailored materials. De Gruyter, Berlin
- Elazzouzi-Hafraoui S, Pataux J-L, Heux L (2009) Self-assembling and chiral nematic properties of organophilic cellulose nanocrystals. *J Phys Chem B* 113(32):11069–11075. <https://doi.org/10.1021/jp900122t>
- Elopak (2021). Range of packages. <https://www.elopak.com/range-of-ambient-packages/>. Accessed 04 Feb 2021
- Fang W, Paananen A, Vitikainen M, Koskela S, Westerholm-Parvinen A, Joensuu JJ, Landowski CP, Penttilä M, Linder MB, Laaksonen P (2017) Elastic and pH-responsive hybrid interfaces created with engineered resilin and

- nanocellulose. *Biomacromol* 18(6):1866–1873. <https://doi.org/10.1021/acs.biomac.7b00294>
- Feng L, Li S, Li Y, Li H, Zhang L, Zhai J, Song Y, Liu B, Jiang L, Zhu D (2002) Super-hydrophobic surfaces: from natural to artificial. *Adv Mater* 14(24):1857–1860. <https://doi.org/10.1002/adma.200290020>
- Footprint® (2019). History of straws: from invention to regulation. <https://footprintus.com/news/sustainability/history-of-straws-from-invention-to-regulation/>. Accessed 04 Feb 2021
- Fortunati E, Peltzer M, Armentano I, Torre L, Jiménez A, Kenny JM (2012) Effects of modified cellulose nanocrystals on the barrier and migration properties of PLA nanobiocomposites. *Carbohydr Polym* 90(2):948–956. <https://doi.org/10.1016/j.carbpol.2012.06.025>
- Fox Jr, TG, Flory PJ (1950). Second-order transition temperatures and related properties of polystyrene. I. Influence of molecular weight. *J Appl Phys* 21(6):581–591. doi:<https://doi.org/10.1063/1.1699711>
- French AD (2017) Glucose, not cellobiose, is the repeating unit of cellulose and why that is important. *Cellulose* 24(11):4605–4609. <https://doi.org/10.1007/s10570-017-1450-3>
- Gao L, McCarthy TJ (2006) Contact angle hysteresis explained. *Langmuir* 22(14):6234–6237. <https://doi.org/10.1021/la060254j>
- Gindl W, Keckes J (2007) Drawing of self-reinforced cellulose films. *J Appl Polym Sci* 103(4):2703–2708. <https://doi.org/10.1002/app.25434>
- Gubskaya AV, Kusalik PG (2002) The total molecular dipole moment for liquid water. *J Chem Phys* 117(11):5290–5302. <https://doi.org/10.1063/1.1501122>
- Habibi Y (2014) Key advances in the chemical modification of nanocelluloses. *Chem Soc Rev* 43(5):1519–1542. <https://doi.org/10.1039/C3CS60204D>
- Hammes MV, Englert AH, Noreña CPZ, Cardozo NSM (2016) Effect of water activity and gaseous phase relative humidity on microcrystalline cellulose water contact angle measured by the Washburn technique. *Colloids Surf A* 500:118–126. <https://doi.org/10.1016/j.colsurfa.2016.04.018>
- Heux L, Chauve G, Bonini C (2000) Nonfloculating and chiral-nematic self-ordering of cellulose microcrystals suspensions in nonpolar solvents. *Langmuir* 16(21):8210–8212. <https://doi.org/10.1021/la9913957>
- Hua Q, Liu L-Y, Karaaslan MA, Rennecker S (2019) Aqueous dispersions of esterified lignin particles for hydrophobic coatings. *Front Chem*. <https://doi.org/10.3389/fchem.2019.00515>
- Hubbe MA, Rojas OJ, Lucia LA (2015) Green modification of surface characteristics of cellulosic materials at the molecular or nano scale: a review. *BioResources* 10(3):6095–6206. <https://doi.org/10.15376/biores.10.3.Hubbe>
- Hult E-L, Ropponen J, Poppius-Levlin K, Ohra-Aho T, Tamminen T (2013) Enhancing the barrier properties of paper board by a novel lignin coating. *Ind Crops Prod* 50:694–700. <https://doi.org/10.1016/j.indcrop.2013.08.013>
- Hutton-Prager B, Adenekan K, Sypnewski M, Smith A, Meadows M, Calicdan C (2021) Hydrophobic development and mechanical properties of cellulose substrates supercritically impregnated with food-grade waxes. *Cellulose* 28(3):1633–1646. <https://doi.org/10.1007/s10570-020-03628-2>
- Indriyati FN, Nuryadin BW, Irmawati Y, Srikandace Y (2020) Enhanced hydrophobicity and elasticity of bacterial cellulose films by addition of beeswax. *Macromol Sympos* 391(1):1900174 1–5. doi:<https://doi.org/10.1002/masy.201900174>
- Jarvis, M C (2018). Structure of native cellulose microfibrils, the starting point for nanocellulose manufacture. *Philos Trans R Soc A: Math Phys Eng Sci* 376(2112): 20170045 1–13. doi:<https://doi.org/10.1098/rsta.2017.0045>
- Joelsson T, Pettersson G, Norgren S, Svedberg A, Höglund H, Engstrand P (2020) High strength paper from high yield pulps by means of hot-pressing. *Nord Pulp Pap Res J* 35(2):195–204. <https://doi.org/10.1515/npprj-2019-0087>
- Kimura S, Laosinchai W, Itoh T, Cui X, Linder CR, Brown RM (1999) Immunogold labeling of rosette terminal cellulose-synthesizing complexes in the vascular plant *vigna angularis*. *Plant Cell* 11(11):2075–2085. <https://doi.org/10.1105/tpc.11.11.2075>
- Korhonen O, Forsman N, Österberg M, Budtova T (2020) Eco-friendly surface hydrophobization of all-cellulose composites using layer-by-layer deposition. *Express Polym Lett* 14:896–907
- Lamb JB, Willis BL, Fiorenza EA, Couch CS, Howard R, Rader DN, True JD, Kelly LA, Ahmad A, Jompa J, Harvell CD (2018) Plastic waste associated with disease on coral reefs. *Science* 359(6374):460–462. <https://doi.org/10.1126/science.aar3320>
- Leal S, Cristelo C, Silvestre S, Fortunato E, Sousa A, Alves A, Correia D, Lanceros-Mendez S, Gama M (2020). Hydrophobic modification of bacterial cellulose using oxygen plasma treatment and chemical vapor deposition. *Cellulose*, 1–14
- Leray C (2007) Waxes. In: Kirk-Othmer (ed) *Kirk-Othmer Encyclopedia of Chemical Technology*, vol 26, 5th edn. Wiley, Hoboken, NJ, pp 203–226
- Lin R, Li A, Zheng T, Lu L, Cao Y (2015) Hydrophobic and flexible cellulose aerogel as an efficient, green and reusable oil sorbent. *RSC Adv* 5(100):82027–82033. <https://doi.org/10.1039/C5RA15194E>
- Lindman B, Karlström G, Stigsson L (2010) On the mechanism of dissolution of cellulose. *J Mol Liq* 156(1):76–81. <https://doi.org/10.1016/j.molliq.2010.04.016>
- Liu K, Du H, Zheng T, Liu W, Zhang M, Liu H, Zhang X, Si C (2021) Lignin-containing cellulose nanomaterials: preparation and applications. *Green Chem* 23(24):9723–9746. <https://doi.org/10.1039/D1GC02841C>
- Ljungberg N, Bonini C, Bortolussi F, Boisson C, Heux L, Cavaillé (2005) New nanocomposite materials reinforced with cellulose whiskers in atactic polypropylene: effect of surface and dispersion characteristics. *Biomacromol* 6(5):2732–2739. <https://doi.org/10.1021/bm050222v>
- Lum K, Chandler D, Weeks JD (1999) Hydrophobicity at small and large length scales. *J Phys Chem B* 103(22):4570–4577. <https://doi.org/10.1021/jp984327m>

- Meador AL, Fries BA (1952) Adsorption in the detergent process. *Ind Eng Chem* 44(7):1636–1648. <https://doi.org/10.1021/ie50511a043>
- Milne AJB, Amirfazli A (2012) The Cassie equation: how it is meant to be used. *Adv Coll Interface Sci* 170(1):48–55. <https://doi.org/10.1016/j.cis.2011.12.001>
- Mohammadi P, Toivonen MS, Ikkala O, Wagermaier W, Linder MB (2017) Aligning cellulose nanofibril dispersions for tougher fibers. *Sci Rep* 7(1):11860. <https://doi.org/10.1038/s41598-017-12107-x>
- Nagalakshmaiah M, El Kissi N, Dufresne A (2016a) Ionic compatibilization of cellulose nanocrystals with quaternary ammonium salt and their melt extrusion with polypropylene. *ACS Appl Mater Interfaces* 8(13):8755–8764. <https://doi.org/10.1021/acsami.6b01650>
- Nagalakshmaiah M, Pignon F, El Kissi N, Dufresne A (2016b) Surface adsorption of triblock copolymer (PEO–PPO–PEO) on cellulose nanocrystals and their melt extrusion with polyethylene. *RSC Adv* 6(70):66224–66232. <https://doi.org/10.1039/C6RA11139D>
- Nageswaran G, Jothi L, Jagannathan S (2019) Chapter 4 - Plasma assisted polymer modifications. In: Thomas S, Mozetič M, Cvelbar U, Špatenka P, Praveen KM (eds) *Non-thermal plasma technology for polymeric materials*, 1st edn. Elsevier, pp 95–127
- Nishiyama Y, Langan P, Chanzy H (2002) Crystal structure and hydrogen-bonding system in cellulose I β from synchrotron X-ray and neutron fiber diffraction. *J Am Chem Soc* 124(31):9074–9082. <https://doi.org/10.1021/ja0257319>
- Nishiyama Y, Sugiyama J, Chanzy H, Langan P (2003) Crystal structure and hydrogen bonding system in cellulose I α from synchrotron X-ray and neutron fiber diffraction. *J Am Chem Soc* 125(47):14300–14306. <https://doi.org/10.1021/ja037055w>
- Notley SM, Norgren M (2010) Surface energy and wettability of spin-coated thin films of lignin isolated from wood. *Langmuir* 26(8):5484–5490. <https://doi.org/10.1021/la1003337>
- Ocean Conservancy (2021) Fighting for trash free seas®. <https://oceanconservancy.org/trash-free-seas/plastics-in-the-ocean/>. Accessed 04 Feb 2021.
- Osong SH, Norgren S, Engstrand P (2016) Processing of wood-based microfibrillated cellulose and nanofibrillated cellulose, and applications relating to papermaking: a review. *Cellulose* 23(1):93–123. <https://doi.org/10.1007/s10570-015-0798-5>
- Österberg M, Vartiainen J, Lucenius J, Hippi U, Seppälä J, Serimaa R, Laine J (2013) A fast method to produce strong NFC films as a platform for barrier and functional materials. *ACS Appl Mater Interfaces* 5(11):4640–4647. <https://doi.org/10.1021/am401046x>
- Ottesen V, Kumar V, Toivakka M, Chinga-Carrasco G, Syverud K, Gregersen ØW (2017) Viability and properties of roll-to-roll coating of cellulose nanofibrils on recycled paperboard. *Nord Pulp Pap Res J* 32(2):179–188. <https://doi.org/10.3183/npprj-2017-32-02-p179-188>
- Panda PK, Jassal M, Agrawal AK (2015) Influence of precursor functionality on in situ reaction dynamics in atmospheric pressure plasma. *Plasma Chem Plasma Process* 35(4):677–695. <https://doi.org/10.1007/s11090-015-9618-9>
- Pang J, Zheng M, Sun R, Wang A, Wang X, Zhang T (2016) Synthesis of ethylene glycol and terephthalic acid from biomass for producing PET. *Green Chem* 18(2):342–359. <https://doi.org/10.1039/C5GC01771H>
- Pankaj SK, Bueno-Ferrer C, Misra NN, Milosavljević V, O'Donnell CP, Bourke P, Keener KM, Cullen PJ (2014) Applications of cold plasma technology in food packaging. *Trends Food Sci Technol* 35(1):5–17. <https://doi.org/10.1016/j.tifs.2013.10.009>
- Petersen RC (1984) The chemical composition of wood. In: Rowell R (ed) *Chemistry of solid wood*, 1st edn. American Chemical Society, pp 57–126
- Popescu M-C, Totolin M, Tibirna CM, Sdrobis A, Stevanovic T, Vasile C (2011) Grafting of softwood kraft pulps fibers with fatty acids under cold plasma conditions. *Int J Biol Macromol* 48(2):326–335. <https://doi.org/10.1016/j.ijbiomac.2010.12.011>
- Qu J, Yuan Z, Wang C, Wang A, Liu X, Wei B, Wen Y (2019) Enhancing the redispersibility of TEMPO-mediated oxidized cellulose nanofibrils in N, N-dimethylformamide by modification with cetyltrimethylammonium bromide. *Cellulose* 26(13):7769–7780. <https://doi.org/10.1007/s10570-019-02655-y>
- Rechendorff K, Hovgaard MB, Foss M, Zhdanov VP, Besenbacher F (2006) Enhancement of protein adsorption induced by surface roughness. *Langmuir* 22(26):10885–10888. <https://doi.org/10.1021/la061923>
- Ren H, Qiao F, Shi Y, Knutzen MW, Wang Z, Du H, Zhang H (2015) PlantBottle™ packaging program is continuing its journey to pursue bio-mono-ethylene glycol using agricultural waste. *J Renew Sustain Energy* 7(4):041510. <https://doi.org/10.1063/1.4929336>
- Ritchie H, Rose M (2018). Plastic pollution. Retrieved 04.02.2021, from <https://ourworldindata.org/plastic-pollution>
- Rodionova G, Lenes M, Eriksen Ø, Gregersen Ø (2011) Surface chemical modification of microfibrillated cellulose: improvement of barrier properties for packaging applications. *Cellulose* 18(1):127–134. <https://doi.org/10.1007/s10570-010-9474-y>
- Ross S, Becher P (1992) The history of the spreading coefficient. *J Colloid Interface Sci* 149(2):575–579. [https://doi.org/10.1016/0021-9797\(92\)90445-R](https://doi.org/10.1016/0021-9797(92)90445-R)
- Salajková M, Berglund LA, Zhou Q (2012) Hydrophobic cellulose nanocrystals modified with quaternary ammonium salts. *J Mater Chem* 22(37):19798–19805. <https://doi.org/10.1039/C2JM34355J>
- Sapieha S, Verreault M, Klemberg-Sapieha JE, Sacher E, Wertheimer MR (1990) X-ray photoelectron study of the plasma fluorination of lignocellulose. *Appl Surf Sci* 44(2):165–169. [https://doi.org/10.1016/0169-4332\(90\)90105-9](https://doi.org/10.1016/0169-4332(90)90105-9)
- Simončič B, Rozman V (2007) Wettability of cotton fabric by aqueous solutions of surfactants with different structures. *Colloids Surf, A* 292(2):236–245. <https://doi.org/10.1016/j.colsurfa.2006.06.025>
- Slavutsky AM, Bertuzzi MA (2014) Water barrier properties of starch films reinforced with cellulose nanocrystals

- obtained from sugarcane bagasse. *Carbohydr Polym* 110:53–61. <https://doi.org/10.1016/j.carbpol.2014.03.049>
- Spence KL, Venditti RA, Rojas OJ, Habibi Y, Pawlak JJ (2010) The effect of chemical composition on microfibrillar cellulose films from wood pulps: water interactions and physical properties for packaging applications. *Cellulose* 17(4):835–848. <https://doi.org/10.1007/s10570-010-9424-8>
- Staudinger VH, In den Birken K-H, Staudinger M (1953) Über den micellaren oder makromolekularen bau der cellulosen. *Die Makromolekulare Chemie* 9(1):148–187. doi:<https://doi.org/10.1002/macp.1953.020090109>
- Tardy BL, Yokota S, Ago M, Xiang W, Kondo T, Bordes R, Rojas OJ (2017) Nanocellulose–surfactant interactions. *Curr Opin Colloid Interface Sci* 29:57–67. <https://doi.org/10.1016/j.cocis.2017.02.004>
- Tardy BL, Mattos BD, Otoni CG, Beaumont M, Majoinen J, Kämäräinen T, Rojas OJ (2021) Deconstruction and reassembly of renewable polymers and biocolloids into next generation structured materials. *Chem Rev* 121(22):14088–14188. <https://doi.org/10.1021/acs.chemrev.0c01333>
- Thomas B, Raj MC, Joy J, Moores A, Drisko GL, Sanchez C (2018). Nanocellulose, a versatile green platform: from biosources to materials and their applications. *Chem Rev* 118(24):11575–11625. doi:<https://doi.org/10.1021/acs.chemrev.7b00627>
- Totolin MI, Vasile C, Tibirna CM, Popescu MC (2008) Grafting of Spanish Broom (*Spartium Junceum*) fibers with fatty acids under cold plasma conditions. *Cellul Chem Technol* 42(7–8):317–333
- Tursi A, De Vietro N, Beneduci A, Milella A, Chidichimo F, Fracassi F, Chidichimo G (2019) Low pressure plasma functionalized cellulose fiber for the remediation of petroleum hydrocarbons polluted water. *J Hazard Mater* 373:773–782. <https://doi.org/10.1016/j.jhazmat.2019.04.022>
- van Heek J, Arning K, Zieffle M (2017) Reduce, reuse, recycle: acceptance of CO₂-utilization for plastic products. *Energy Policy* 105:53–66. <https://doi.org/10.1016/j.enpol.2017.02.016>
- Wahba, M and Nashed, S (1957). 1—Moisture relations of cellulose. III. Sorption hysteresis and the effect of temperature. *J Text Inst Trans* 48(1):T1–T20. doi:<https://doi.org/10.1080/19447025708659748>
- Walker J (2006) *Primary wood processing: principles and practice*. Springer
- Wang J, Cheng Q, Lin L, Jiang L (2014) Synergistic toughening of bioinspired poly(vinyl alcohol)–clay–nanofibrillar cellulose artificial nacre. *ACS Nano* 8(3):2739–2745. <https://doi.org/10.1021/nn406428n>
- Wang T, Zhao Y (2021) Fabrication of thermally and mechanically stable superhydrophobic coatings for cellulose-based substrates with natural and edible ingredients for food applications. *Food Hydrocolloids* 120:106877. doi:<https://doi.org/10.1016/j.foodhyd.2021.106877>
- Wei L, Agarwal UP, Matuana L, Sabo RC, Stark NM (2018) Performance of high lignin content cellulose nanocrystals in poly(lactic acid). *Polymer* 135:305–313. <https://doi.org/10.1016/j.polymer.2017.12.039>
- Wenzel RN (1936) Resistance of solid surfaces to wetting by water. *Ind Eng Chem* 28(8):988–994. <https://doi.org/10.1021/ie50320a024>
- White LR (1977) On deviations from Young’s equation. *J Chem Soc Faraday Trans 1: Phys Chem Condens Phases* 73(0):390–398. doi:<https://doi.org/10.1039/F19777300390>
- Whyman G, Bormashenko E, Stein T (2008) The rigorous derivation of Young, Cassie–Baxter and Wenzel equations and the analysis of the contact angle hysteresis phenomenon. *Chem Phys Lett* 450(4):355–359. <https://doi.org/10.1016/j.cplett.2007.11.033>
- Wolansky G, Marmur A (1999) Apparent contact angles on rough surfaces: the Wenzel equation revisited. *Colloids Surf, A* 156(1):381–388. [https://doi.org/10.1016/S0927-7757\(99\)00098-9](https://doi.org/10.1016/S0927-7757(99)00098-9)
- Xhanari K, Syverud K, Chinga-Carrasco G, Paso K, Stenius P (2011) Reduction of water wettability of nanofibrillated cellulose by adsorption of cationic surfactants. *Cellulose* 18(2):257–270. <https://doi.org/10.1007/s10570-010-9482-y>
- Yamane C, Aoyagi T, Ago M, Sato K, Okajima K, Takahashi T (2006) Two different surface properties of regenerated cellulose due to structural anisotropy. *Polym J* 38(8):819–826. <https://doi.org/10.1295/polymj.PJ2005187>
- Yasuda T, Okuno T, Yasuda H (1994) Contact angle of water on polymer surfaces. *Langmuir* 10(7):2435–2439. <https://doi.org/10.1021/la00019a068>
- Young T (1805) III. An essay on the cohesion of fluids. *Philos Trans R Soc Lond* 95:65–87. <https://doi.org/10.1098/rstl.1805.0005>
- Zhang J (2022) Application of cold plasma in food packaging. In: Ding T, Cullen PJ, Yan W (eds) *Applications of cold plasma in food safety*, 1st edn. Springer Singapore, Singapore, pp 309–324
- Zhang X, Huang H, Qing Y, Wang H, Li X (2020) A comparison study on the characteristics of nanofibrils isolated from fibers and parenchyma cells in bamboo. *Materials* 13(1):237
- Zhang W, Lu P, Qian L, Xiao H (2014) Fabrication of superhydrophobic paper surface via wax mixture coating. *Chem Eng J* 250:431–436. <https://doi.org/10.1016/j.cej.2014.04.050>
- Zhao D, Tian Q, Wang M, Jin Y (2014) Study on the hydrophobic property of shark-skin-inspired micro-riblets. *J Bionic Eng* 11(2):296–302. [https://doi.org/10.1016/S1672-6529\(14\)60046-9](https://doi.org/10.1016/S1672-6529(14)60046-9)
- Zhao Y, Moser C, Henriksson G (2018) Transparent composites made from tunicate cellulose membranes and environmentally friendly polyester. *Chemoschem* 11(10):1728–1735. <https://doi.org/10.1002/cssc.201800627>
- Zille A, Oliveira FR, Souto AP (2015) Plasma treatment in textile industry. *Plasma Processes Polym* 12(2):98–131. <https://doi.org/10.1002/ppap.201400052>

Publisher’s Note Springer Nature remains neutral with regard to jurisdictional claims in published maps and institutional affiliations.